Acta Geotechnica (2020) 15:1341–1361
https://doi.org/10.1007/s11440-019-00810-0

SHORT COMMUNICATION

Field monitoring of suction in the vicinity of an urban tree: exploring termite infestation and the shading effects of tree canopy

Wan-Huan Zhou[1] · Shu-Yu He[2] · Ankit Garg[3] · Zhen-Yu Yin[4]

Received: 16 July 2018 / Accepted: 5 April 2019 / Published online: 11 May 2019

Abstract

The objective of this short communication is to explore spatial distribution of soil suction in the vicinity of an urban tree considering effects of termite infestation and also radiant energy interception by canopy. A site in an urban landscape containing a mix of species cover (grass cover in the vicinity of trees) was selected for monitoring. A field monitoring program was designed to monitor soil (soil suction, moisture), vegetation parameters (tree height, grass leaf area), and meteorological parameters during drying/wetting cycles. As expected, before termite infestation, suction magnitude and rate of change were highest near the tree stem and at shallower depths, reflecting the dominance of transpiration over evaporation. However, after termite infestation, soil suction diminished significantly near the tree stem and increased farther from the tree stem, a phenomenon accompanied by loss of canopy area, as captured by a color analysis technique (i.e., an image processing method). These findings reflected a reduction in stomatal conductance, itself an indicator of transpiration loss through the stomata—likely because reduced canopy shading effects caused increased evaporation. Soil suction at deeper depths seemed not to be significantly affected, generally due to canopy and termite infestation. In summary, the study sheds new light on issues of tree maintenance by showing how termite infestation can significantly affect the performance of green infrastructure.

Keywords Soil suction · Stomatal conductance · Termite infestation · Tree canopy · Urban landscape

1 Introduction

Numerous studies have demonstrated the hydrological effects (i.e., soil moisture and soil suction) induced by vegetation from the perspectives of slope stability [17, 19–24, 42, 46, 51, 56, 60, 61] and agricultural crop yield [5, 41, 53, 55]. An understanding of soil–plant–atmospheric interactions is crucial for analysis of such hydrological responses, with recent studies [15–17, 19, 20, 50] having demonstrated the effects of canopy properties (i.e., leaf area index), root properties (i.e., root area index), and tree/grass mix interactions in the soil–plant–atmospheric continuum. These interactions have been found to significantly affect hydrological responses (such as infiltration) [17] from vegetation across seasons.

Both the presence of buildings in the urban landscape and the presence of the plant canopy may cause shading effects [17] by intercepting incoming radiant energy required for photosynthesis and transpiration of vegetation, which in turn can influence root water uptake. Whereas

✉ Ankit Garg
ankit@stu.edu.cn

Wan-Huan Zhou
hannahzhou@um.edu.mo

Shu-Yu He
heshuyu94@gmail.com

Zhen-Yu Yin
zhenyu.yin@polyu.edu.hk

[1] State Key Laboratory of Internet of Things for Smart City and Department of Civil and Environmental Engineering, University of Macau, Macau S.A.R., China

[2] Department of Civil and Environmental Engineering, Faculty of Science and Technology, University of Macau, Macau, China

[3] Department of Civil and Environmental Engineering, Shantou University, Shantou 515063, Guangdong, China

[4] Department of Civil and Environmental Engineering, Hong Kong Polytechnic University, Hung Hom, Kowloon, Hong Kong, China

interception by the tree canopy can enhance soil suction [19, 42, 59], interception by buildings in the urban environment can degrade suction. Hence, interception of radiant energy plays an important role in analysis of hydrological responses from vegetation in an urban landscape. Likewise, an understanding of water flow in an urban green infrastructure is necessary for design or analysis of vegetation in the urban landscape. Some studies [12, 25, 34] have reported differential settlement caused by water uptake or preferential flow under rain due to the presence of vegetation roots near buildings in the urban landscape. Furthermore, the presence of mixed species (grass and trees) in a green infrastructure may cause heterogeneity in the distribution of radiant energy [35], of vegetation growth, and hence of soil suction, which should be further quantified. Various studies [30, 40, 47, 54, 57] have noted that solar elevation angle varies with seasons, affecting distribution of radiant energy on the ground as well as shading portions, with the solar elevation angle generally higher in summer than in winter. Accordingly, radiant energy distribution varies significantly with solar angle and with the position of elements such as buildings. For these reasons, solar elevation angle is a primary consideration in the urban landscape, where shading effects are likely to be amplified.

Another important ecological process that has been reported to influence the water soil–plant–atmospheric continuum is the presence of a termite colony (Fig. 1). Termites usually feed on live or dead vegetation, consuming cellulose from wood. Termite infestations are a major cause of tree death in urban environments compared to forests [13, 27, 28, 37, 45], in part because of urban planners' failure to select plant species suitable for a site and lack of care when transplanting the trees, factors exacerbated by the lack of space for plant growth in the urban environment. Termites influence the spatial distribution and dynamics of soil as well as of vegetation [9, 13, 28, 32, 37, 45], with the water flow mechanism in an engineering infrastructure infected by termites able to influence the water uptake process of vegetation and hence soil suction.

All these interactions of urban elements and ecological processes (such as termite colony feeding) call for further investigations of the soil–plant–atmospheric continuum with a view to designing better urban infrastructure. For example, an understanding of the influence zone of suction (spatial variations) induced around a tree in an urban landscape featuring mixed grass species and tree–grass interactions could help engineers and architects improve their planning of infrastructure. In addition, meteorological parameters have been found to significantly affect various activities of vegetation [26], such as photosynthesis, respiration, and transpiration. Because these meteorological parameters can vary locally with the presence or absence of certain elements of the urban landscape (buildings, canopies of other species, etc.), comprehensive study is needed of hydrological responses from mixed vegetation (tree and grass cover) in an urban landscape.

The main objective of this study is to explore spatial distribution of soil suction in the vicinity of an urban tree considering effects of termite infestation and also radiant energy interception by canopy. In this study, site containing vegetation such as "*Elaeocarpus Apiculatus Master*" and "*Pink Shower Tree*" was selected for investigation. These trees were selected for investigation, as they are commonly found in the subtropical regions including many parts of India, China, and Japan. In addition, they have contrasting feature, i.e., the former is evergreen tree, while the latter is deciduous tree A field monitoring program was conducted to investigate spatial variations in soil suction,

Fig. 1 Termites feed on the cellulose in the wood of a tree stem and ultimately influence the tree's growth (accessed from website: https://rainforestpartnership.org/termites-the-rainforest-protector/)

radiant energy, and plant parameters. Instrumentation was specifically planned to measure suction at different distances from tree stem or canopy (i.e., at different extent of tree–grass interaction). Using a simple shear strength equation, the significance of measured suction in the urban landscape near and far from a tree was evaluated. Finally, a comparison was made with other studies involving relatively remote landscapes (slopes, agricultural fields).

2 Materials and methods

2.1 Site description

A site for field monitoring was selected on the new campus of the University of Macau (UM), on Hengqin Island, Zhuhai, China. This site was selected because the campus landscape resembles a typical urban landscape.

Figure 2 shows the location of the field monitoring site. The average daily temperature was obtained from Macao Meteorological and Geophysical Bureau. The average daily temperature was calculated by estimating the mean of daily average temperatures during the monitoring period. The average temperature in Macau during the monitoring period was 22.3 °C, with the highest temperature 36.1 °C and the lowest 5.0 °C. The average relative humidity was relatively high at about 80%, and cumulative rainfall was 2,058.1 mm. The field monitoring site is located just near the river in the urban landscape of the University of Macau campus. The ground water table (GWT) at this site is located about 1.5 m below the ground surface.

2.2 Field monitoring

Field monitoring was conducted in an urban landscape (Fig. 3a) on the University of Macau campus from October 7, 2016, to September 1, 2017, a timeframe sufficient to allow measurement of a wide range of soil suction magnitudes (i.e., from 0 to 637.4 kPa; Fig. 12) and meteorological parameter values (Fig. 7a–c) around the vicinity of the tree. So long a monitoring period provided sufficient variation in measurement points around the tree's vicinity to allow quantification of the spatial distribution of suction (or influence zone). The monitoring period was divided

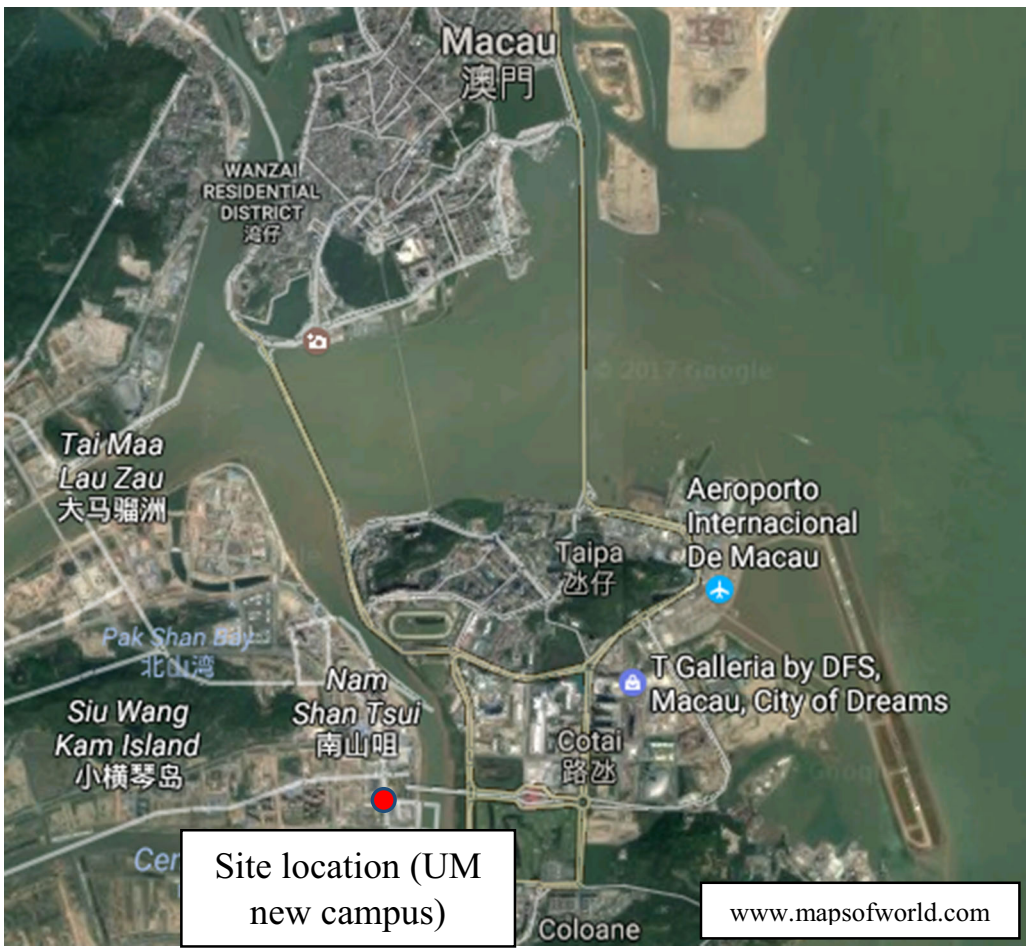

Fig. 2 Location of the field test site on the University of Macau campus, Macau, China

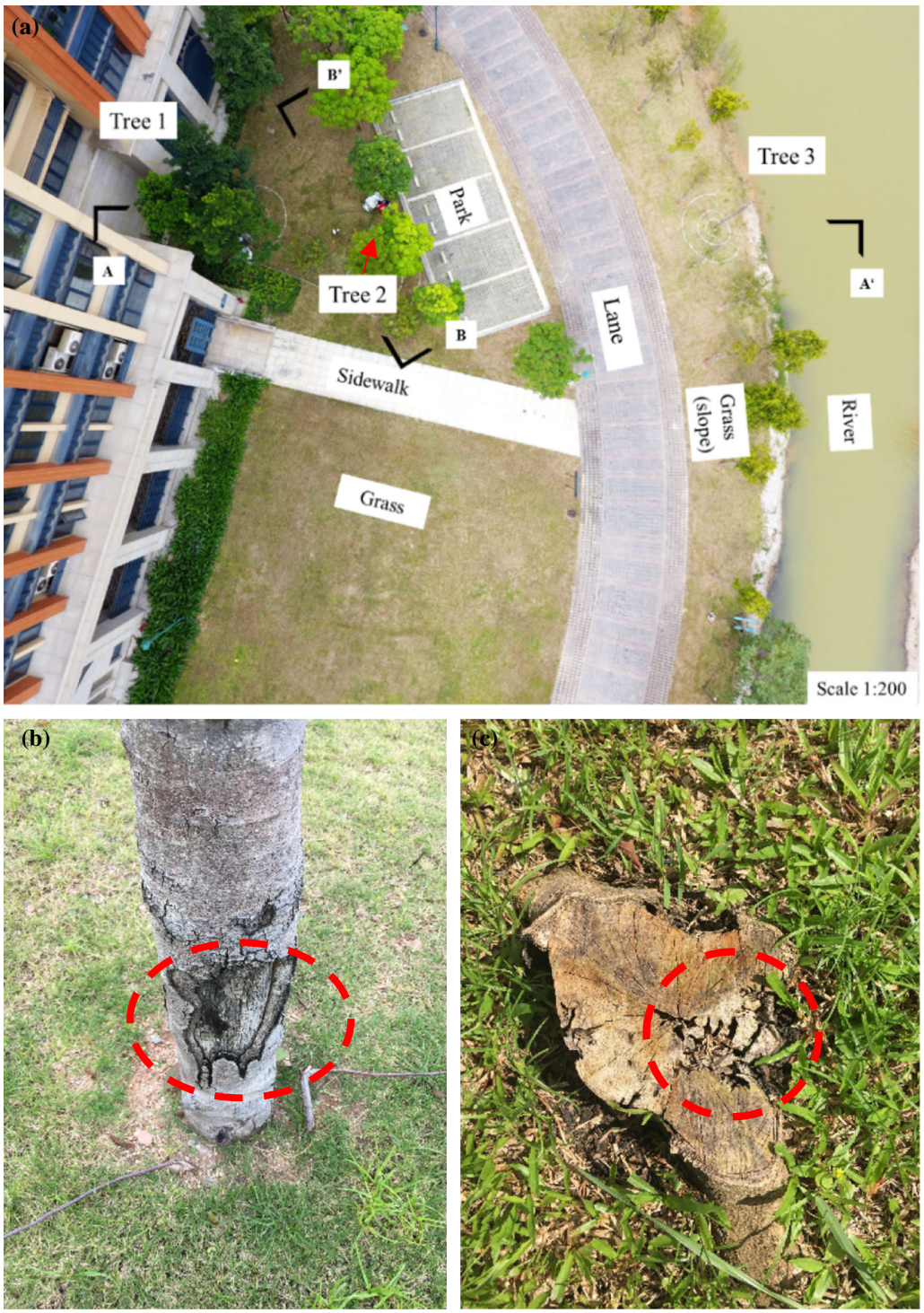

Fig. 3 Field monitoring site and infected tree: **a** overhead view of selected testing site showing overview of instrumentation for measuring suction and soil moisture in a mixed-species site (tree–grass interactions); **b** termite infestation of T2; **c** stem of T2 after its removal by campus grounds management after the monitoring period. Red circles show the infested portions of the tree (color figure online)

into two stages distinguished by the onset of a termite infestation in the tree (discussed later). Stage 1 included monitoring from October 7, 2016, to May 31, 2017, and stage 2 included monitoring from June 1 to September 1, 2017.

Instrumentation design was intended to bring an understanding of variations in soil suction around the

vicinity of a tree in a mixed-species site (i.e., tree–grass interactions). This was done by fixing a reference line (Fig. 3a; bird's-eye view of selected site using UAV [DJI Phantom 4]) far from the main tree under investigation. Soil suction and radiant energy distribution were investigated at different distances from the tree. To measure a wide range of suctions (i.e., from 0 kPa to more than 100 kPa), two different instrumentations were used. Jet fill tensiometers (Soil Moisture Equipment Corp., 2010) were used to measure suctions below 90 kPa; for suctions above 90 kPa, dielectric water potential sensors (MPS sensors [8]) were used, considering Tripathy et al.'s [52] finding that MPS sensors can measure from 10 kPa to 10,000 kPa of suction.

Three trees were selected as research subjects: Tree 1 (T1), Tree 2 (T2), and Tree 3 (T3). T1 and T2 were both of the species *Elaeocarpus Apiculatus Master*, whereas T3 was of the species *Pink Shower Tree*. This study examined spatial variations in the suction around the vicinity of T2 while seeking to understand how the presence of different species, such as T3, would affect suction. During the monitoring period, T2 was observed to be infested with termites, as shown in Fig. 3b. The site of infestation was clearly visible, as shown by the red circles in Fig. 3b, c, before and after the tree's cutting, respectively. Previous field studies that have analyzed the effects of termite infestations on vegetation dynamics [11, 36] have found that termites usually feed on woody plants, leaves, and litter, as well as sometimes also on dead vegetation. During our field monitoring, we also analyzed variations in suction and moisture in the soil over time for T2, expecting a decline in vegetation growth with worsening of the termite infestation.

2.3 Instrumentation

Figure 4 presents a cross-sectional view of the instrumentation used. As shown in Fig. 4a, sensors for measuring suction were installed at three depths (0.2 m, 0.4 m, 0.6 m). At the shallowest depth, dielectric water potential sensors were installed. Sensors (both soil suction and soil moisture) were installed at 0.2 m depth. This particular depth was selected as it lies within the range of transplanted tree root zone (0.3–0.5 m). Significant development of soil suction is expected due to rapid loss of water near the surface through evapotranspiration from grass roots. The particular sensor will be able to capture the effects of tree roots. Previous studies [6, 43, 48, 49] also observed variations in soil moisture at shallower depths for *Schefflera heptaphylla*. At the deeper depths, where expected suction was lower (< 90 kPa), jet fill tensiometers were installed. To quantify the lateral influence of the zone of suction, a similar set of suction probes along depth were installed at four different distances from the stem: point A (0.5 m from the tree stem), point B (1.5 m), point C (3 m), and point D (5.5 m). These points were selected to ensure coverage within the canopy as well as outside it, the better to quantify intercepted radiant energy effects. In addition, the instruments for measuring soil suction and moisture were carried out along lines at farthest distances (3–4 m) from other trees. This was done to ensure minimum interactive of trees [31]. It is assumed in this study that the effects of interaction among trees on soil suction/moisture measurements are negligible. Further studies are required to analyze group interaction effects of trees on soil suction. For installing soil moisture and suction sensors, a careful procedure was adopted. Before installing Jet fill tensiometer, a kaolin paste was applied to porous tip. This was to ensure proper contact between soil particles and porous tip. The Jet fill tensiometer was also saturated before inserting it into ground. After insertion of Jet fill tensiometer to a required depth, the space around tensiometer was filled with soil to remove any air gap. Further, the area around the Jet fill tensiometer (at ground surface) was cemented to minimize any preferential flow. For MPS-6 sensors, a similar procedure was adopted but without any need of saturation. For soil moisture probes, after inserting the sensors the hole was backfilled and a cement paste is applied around the wire (at ground surface), to minimize any preferential flow of water.

Figure 4b shows a cross-section of the site in another direction (A–A′ section), with two more points (point F near T1, point E near T3) selected to aid study of the effects of nearby urban landscape (i.e., river and building).

Because interpretation of suction distribution under varying natural conditions requires close monitoring of environmental parameters, a microclimate monitoring station [7] was installed to measure rainfall intensity (rain gauge), air humidity (VP-3 sensor), temperature (VP-3 sensor), and radiant energy (quantum meter). When measuring the spatial distribution of radiant energy (including intercepted energy), measurements made using the quantum meter were obtained at several points within the canopy of the tree as well as outside it. Solar elevation angle was calculated using the computer program NOAA, based on Astronomical Algorithms, by Jean Meeus (Earth System Research Laboratory), which gives correct times for sunset and sunrise to within 1 min for locations within the latitudes ± 72°. (Due to variations in atmospheric conditions, observed values may differ from calculated ones.) Solar elevation angle, the angle between the incidence direction of sunlight and the horizon, is significant in the urban landscape for indicating what fraction of total radiation will reach ground level. Theoretically, solar radiation increases with increased solar angle: when solar

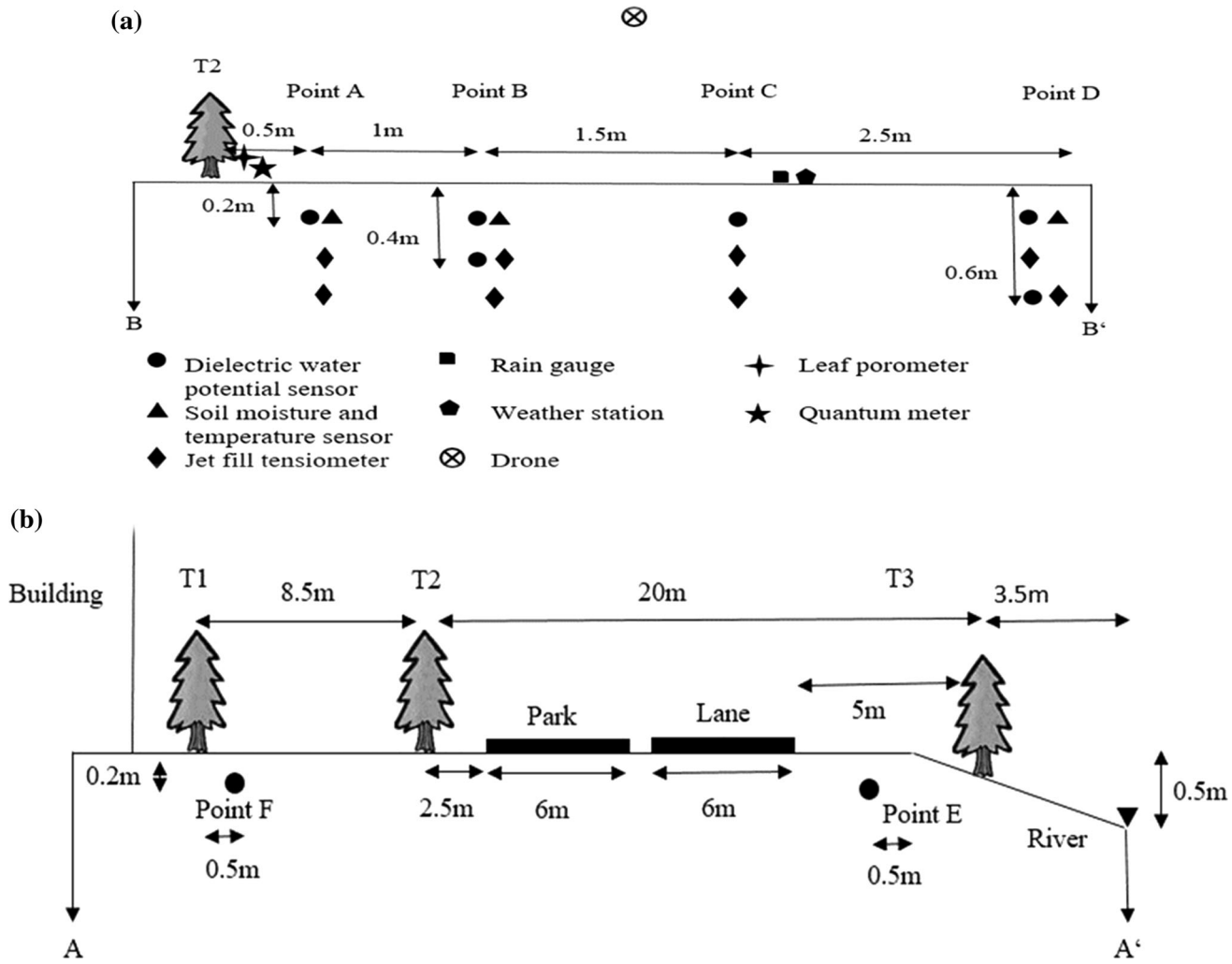

Fig. 4 Sensor instrumentation plan

elevation angle reaches 90°, solar radiation has reached its highest value.

2.4 Image analysis of canopy cover

Image segmentation can aid identification of tree canopy cover in an urban landscape featuring a mix of trees, grass, and other elements. Image J is an open-source program that allows users to carry out image segmentation [17]. The images of trees were captured using UAV. For capturing the tree canopy cover, UAV was positioned at a height (i.e., 20 m above ground). The position was fixed so as to ensure consistency of images to be captured at different time intervals. The images were taken at mid-day (around 1 PM), which usually corresponds to maximum light intensity or radiant energy. The images were mainly captured on a less cloudy day to ensure proper lighting and hence for capturing high resolution images. Detailed procedures have also been mentioned in Gadi et al. [16, 17].

Color threshold was used as the method of image segmentation, with the procedures used for this conversion adopted from Gadi et al. [17], in which various patches of grass cover were analyzed under different shading conditions. Their study quantified different fractions of grass cover with respect to time and space in a mixed-vegetation site, separating each of the RGB components of an image according to its distinctive features (tree, river, grass cover, etc.; Fig. 5). In this study, the HSB (hue, saturation, and brightness) color space was adopted for its ability to remove unnecessary color (only green is needed to analyze a plant canopy) by adjusting the value of hue. Using an adjusted constant value of HSB, only a few noise points (pixels associated with similarly colored objects) would remain after setting the color threshold.

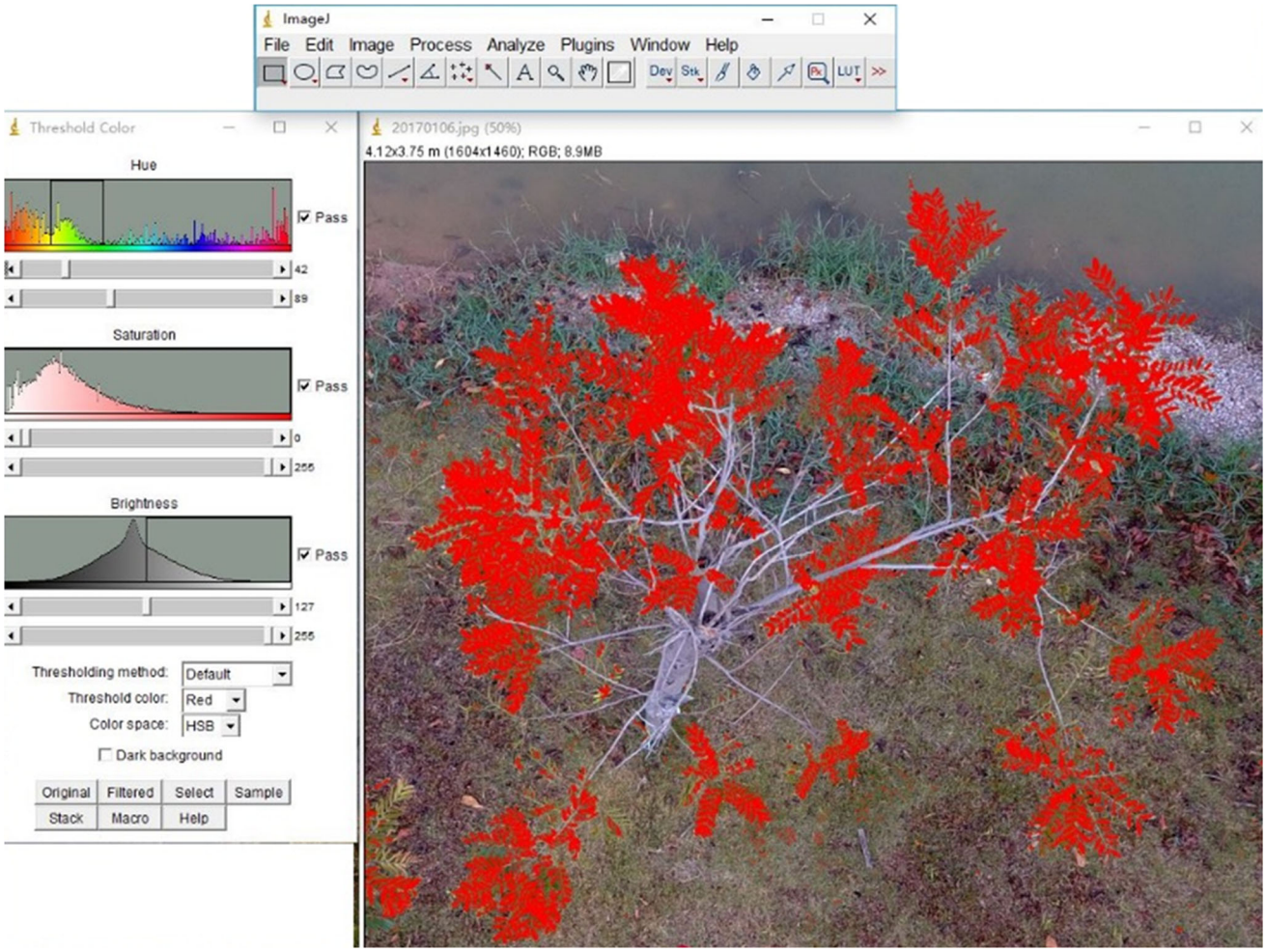

Fig. 5 Image analysis after image segmentation

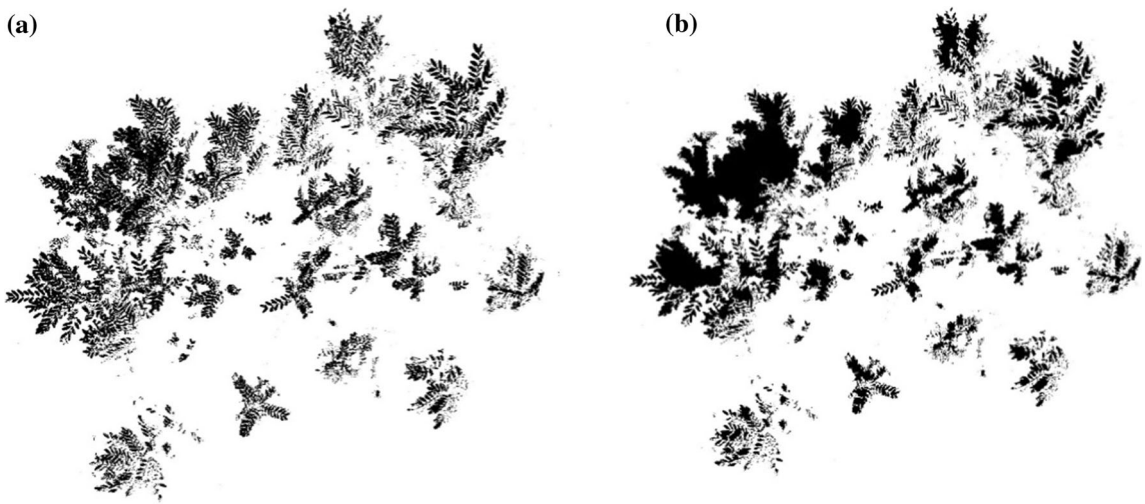

Fig. 6 Binary images of T3 captured on January 9, 2017, **a** before and **b** after applying a fill holes filter

After removing the noise points, the scale of the image was calibrated with the known dimensions of the object in its site. In this study, a circular mark around the tree's vicinity was used, much as in the study by Gadi et al. [17]. Next the image was converted into a binary image (Fig. 6) for calculation of black areas.

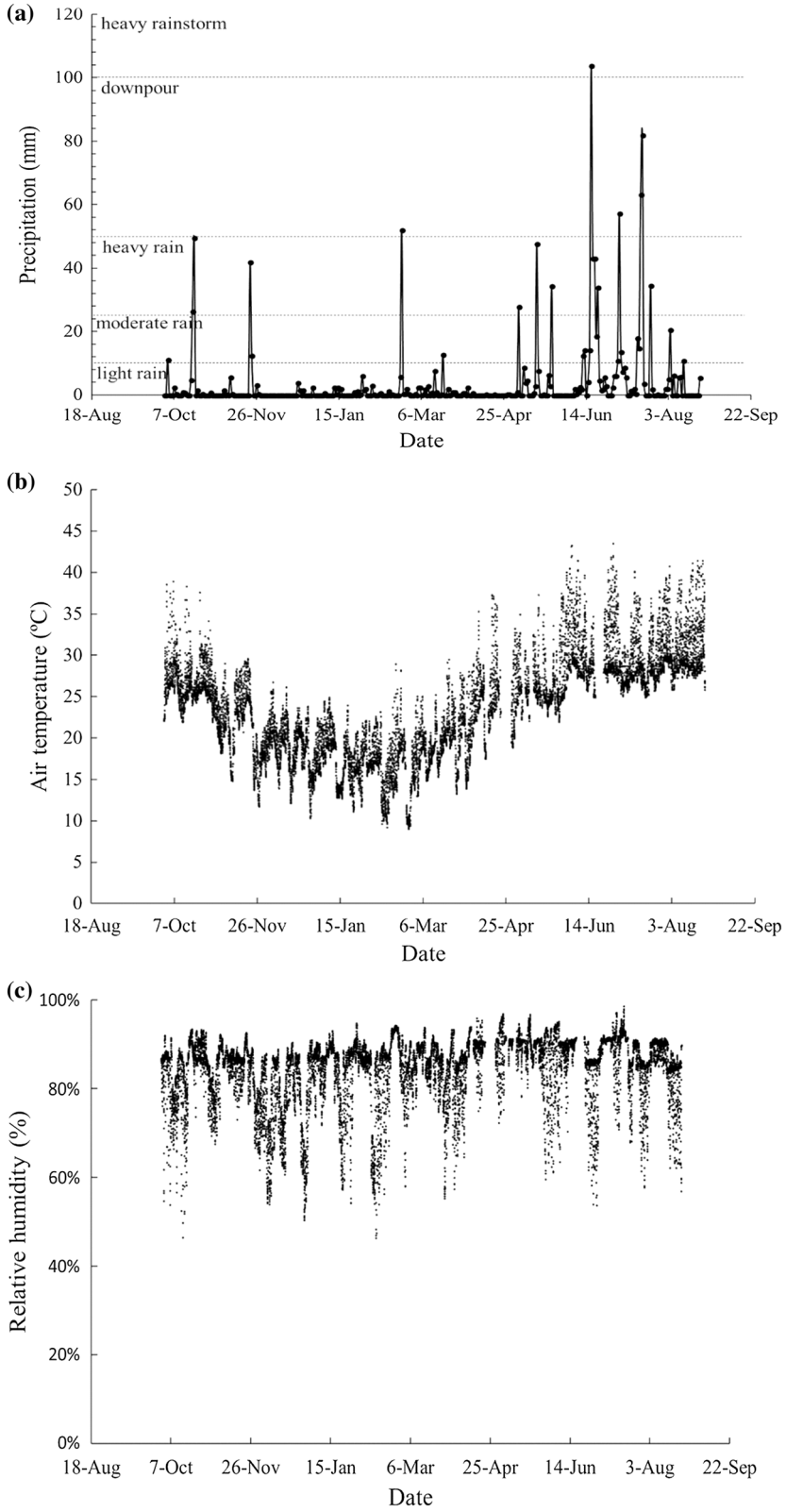

Fig. 7 Variations in meteorological parameters: **a** rainfall, **b** air temperature, and **c** relative humidity

The fill holes function was used to minimize discrepancies resulting from differing light conditions [18]. This function built into Image J fills small and closed circles in a binary image after image segmentation (Fig. 6b). Similar procedures were applied for Tree 2 to capture total canopy area at different intervals during the monitoring period.

3 Results and discussion

3.1 Meteorological parameters in the urban landscape during the field test period

Figure 7a–c shows variations in meteorological parameters such as precipitation (daily rainfall), air temperature, and relative humidity during the monitoring period. It can be seen from Fig. 7a that the monitoring period saw frequent rainfall events, with maximum daily rainfall ranging from 0 to 103 mm. The peak daily rainfall was observed on June 14, 2017. Generally, rainfall amount and frequency were both lower for the period from October to May than for the period from May to September, reflecting the shift of season from winter to summer. Air temperature (Fig. 7b) rose gradually with that same shift. Also, air temperature fluctuated during day and night periods, dropping from over 40 °C at the beginning of October to around a minimum of 10 °C at the beginning of March and then rising to around 40 °C once more at the end of September.

Relative humidity (RH) fluctuated between 50 and 90% during most of the monitoring period, with differences in relative humidity between winter and summer not as significant as those between air temperature and rainfall. Variations in rainfall and air temperature thus might have exerted more influence on evapotranspiration (per the equation proposed by Allen et al. [1]) and hence induced suction, although changes in relative humidity are also significant for causing variations in evaporation- or evapotranspiration-induced soil suction, per Kelvin's equation.

3.2 Radiant energy characteristics of the urban landscape during the field test period

Radiant energy characteristics such as solar elevation angle and radiant energy magnitude (μmol/m^{2}s) were quantified while remembering the importance of solar elevation angle, indicating as it does the direction of the sun's inclination, in the urban landscape for its influence on the degree of shade caused by elements such as tree canopy and buildings. A clear understanding of solar elevation angle can aid exploration of the shading effects of buildings near selected trees (especially Tree T2).

To elucidate the effects of variations in solar radiation, the solar elevation angle (Fig. 8) was calculated for the year 2016. According to the NOAA solar position calculator (Earth System Research Laboratory), the solar elevation angle at 10 a.m. varied from around 20° in December to around 40° in June. Solar elevation angle increases with the change in season from winter to summer, indicating that the intensity and radiant energy of sunlight are likely to be at their minimum during winter and at their

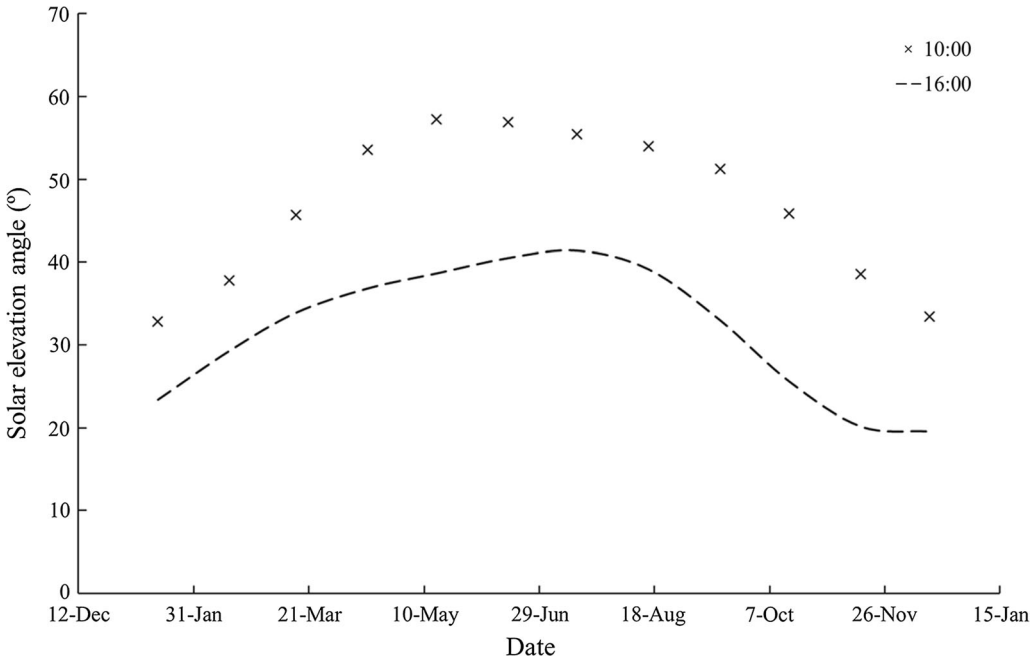

Fig. 8 Variations in solar elevation angle in 2016 (calculated using the NOAA solar position calculator H.K.)

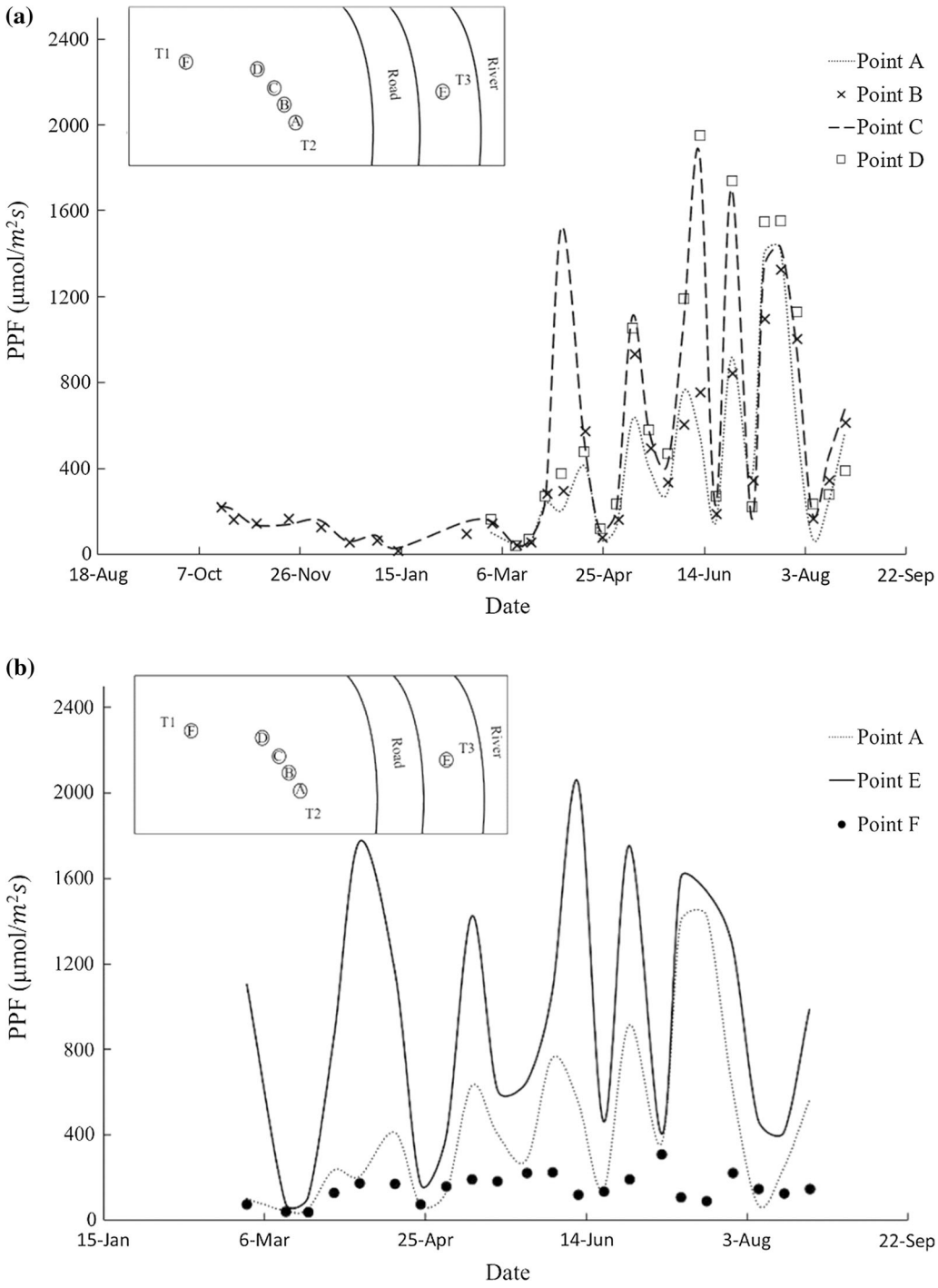

Fig. 9 Variations in PPF at **a** different distances from tree stem and **b** isolated points away from tree stem during the monitoring period

maximum during summer [47]. The significance of solar elevation angle on radiant energy distribution in the presence of a tree or building in an urban area can be further understood from Fig. 9.

To provide an understanding of the effect of tree canopy on the urban landscape, measurements of radiant energy (at 10 a.m. and 4 p.m.) at four different points (see Fig. 4) were plotted over time. Figure 9a, b shows variations in the soil surface's received radiant energies at four points at different distances from T2 (A, B, C, D) and three points under T2 shade (A), building shade (F), or no shade (E). All measurements were taken at 10 a.m. and 4 p.m., the times when radiant energy is likely to be at its extremes. Figure 9a shows an increase in radiant energy with increased distance from tree stem (T2), likely because the interception effects of the tree canopy decrease with

distance from tree stem. Similar observations were made by Garg et al. [19] in a relatively smaller test setup in a laboratory for a tree seedling, *Schefflera heptaphylla*. Notably, radiant energy at 10 a.m. was greater than that seen at 4 p.m., perhaps because of the lowered elevation angle of the sun by that time.

Figure 9b shows that point E, free of tree and building shading effects, received the highest level of radiant energy at 10 a.m., whereas point F (near a building) received the lowest level of radiant energy at both 10 a.m. and 4 p.m., implying that shade effects from the adjacent building were effective throughout the day. Radiant energy for point A (close to T2) lay between that for points A and F. Thus, in general, radiant energy increased with distance from the building (from point F to point E). The distribution of radiant energy on the ground as a result of interception by buildings or trees may affect suction distribution, a possibility that will be discussed later.

3.3 Plant growth

This section presents an analysis of plant parameters, including canopy area, canopy diameter, and root spread.

3.3.1 Plant activity

Tables 1 and 2 summarize the data produced by image analysis of the canopy area, canopy diameter (see Sect. 2.4) and also leaf area index (LAI). LAI is estimated based on simplified definition (Ni et al., 2018) by dividing the total area of leaves with the canopy diameter. The canopy diameter is defined as the distance between two farthest (diametrically opposite) leaves on tree. It is calculated using image analysis [44]. In January, 3 days were selected for this comparison, with analysis finding only slight fluctuations after use of the fill holes function.

Table 1 Leaf area and canopy diameter of T2

Date	Leaf area (m^2)	Canopy diameter (m)	Leaf area index (LAI)
2017/01/05	13.11	4.53	0.81
2017/01/09	13.06	4.46	0.83
2017/01/13	13.23	4.56	0.81
2017/02/12	13.57	4.50	0.85
2017/03/01	13.78	4.61	0.82
2017/03/16	14.26	4.49	0.90
2017/04/28	13.55	4.63	0.80
2017/05/12	13.32	4.58	0.80
2017/07/04	7.13	4.3	0.49
2017/08/09	7.23	4.36	0.48
2017/09/14	0.563	2.93	0.08

Table 2 Canopy area and canopy diameter of T3

Date	Leaf area (m^2)	Canopy diameter (m)	Leaf area index (LAI)
2017/01/05	2.04	2.30	0.491253
2017/01/09	2.01	2.34	0.467622
2017/01/13	1.99	2.32	0.470985
2017/02/12	2.20	2.33	0.516228
2017/03/01	2.18	2.40	0.48213
2017/03/16	2.20	2.32	0.520687
2017/04/28	2.62	2.26	0.653454
2017/05/12	2.50	2.35	0.57668
2017/07/04	2.18	2.45	0.462652
2017/08/09	2.12	2.39	0.472792
2017/09/14	0	2.11	0

As observed from Table 1, the LAI for tree T2 was approximately around 0.8 from January 5, 2017, till May 2017. Further, as observed from the table, the LAI reduced significantly beyond May 2017. This is likely because of termite infestation (Fig. 3b, c). On the other hand, LAI of tree T3 is even lower than that of T2. This indicates that tree T3 has even less dense leaf arrangement. On the contrary to T2, there is no sharp decline in LAI beyond May. However, after the tree was cut, the LAI was assumed to be 0 in September 2017. Notably, T3 (refer to Table 2) did not see such a decline beyond May 3.

Another parameter that can also reflect vegetation growth is stomatal conductance (μmol/m^2s), which is generally measured using a leaf porometer. Figure 11 shows the variation in stomatal conductance of T2's leaves during the monitoring period. Generally, the stomatal conductance values for tree T2 varied at around 10 μmol/m^2 s or below, with the literature [2, 14] indicating that these values might be at least 10 times lower for an infested tree species. This might be because of the different soil conditions and lack of organic content that differentiate the urban landscape from that of a forest [4, 33]. The artificial soil seen in the urban landscape is often devoid of the soil microbial communities that are essential for sustaining vegetation growth [29, 38]. Presence of shredded leaves and earthworms makes soil more porous and provides a better habitat for soil-dwelling microorganisms than urban soils can. In urban soils, moreover, artificial pest management practices may reduce microorganism growth still further. For these reasons, higher levels of stomatal conductance are seen in forest trees than in urban trees.

Stomatal conductance values declined from their maximum of approximately 10 μmol/m^2s in January 2017 to around 4 μmol/m^2 s by the end of April 2017. This decline was unexpected, as climate conditions such as radiant

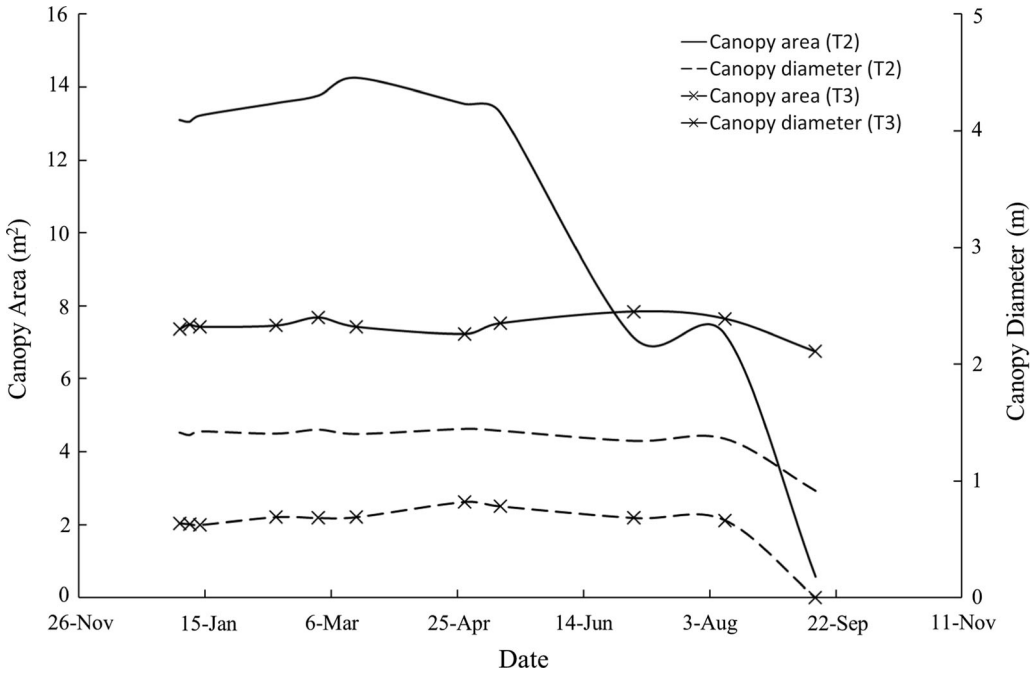

Fig. 10 Variations in canopy area and canopy diameter during the field test period

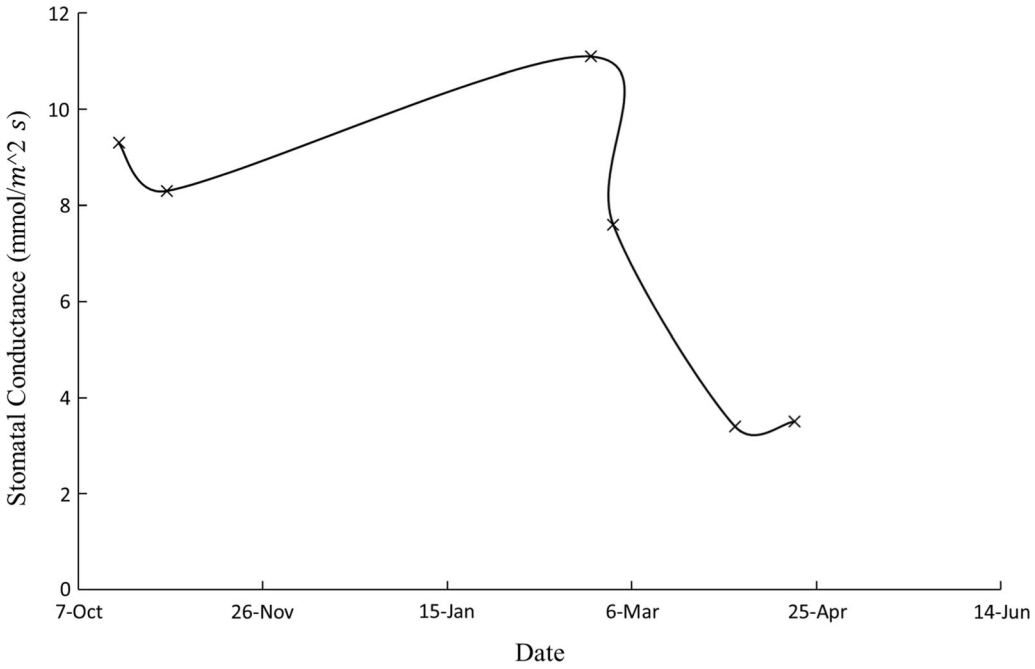

Fig. 11 Variations in stomatal conductance at several times during the monitoring period

energy and air temperature seemed to be more favorable for vegetation photosynthesis and transpiration [39] in April than in January. The timeline for T2's decline in stomatal conductance appears to be similar to that for its leaf area (Fig. 10).

3.3.2 Measured lateral extent of roots and trunk diameter

Borehole tests were conducted to analyze the lateral extent of roots for all the trees. Lateral spread of roots for T1, T2, and T3 were found as 4 m, 4.5 m, and 3.7 m, respectively.

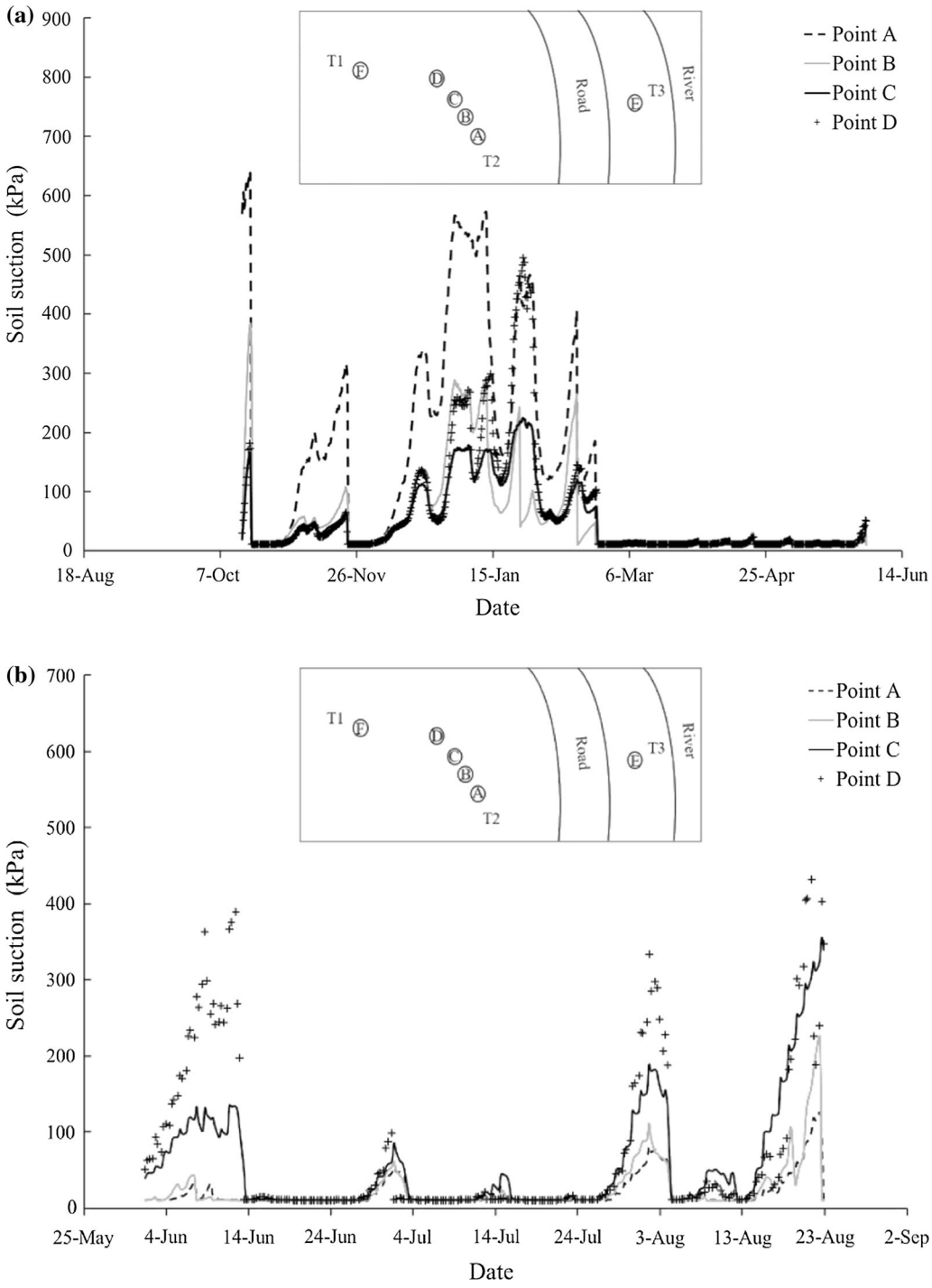

Fig. 12 Variations in soil suction at 20 cm depth during **a** stage 1 and **b** stage 2 of monitoring period

Based on the results of analysis and measurement, the height of T1, T2, and T3 are 13 m, 11 m, and 8 m, respectively. Trunk diameters is usually measured at breast height [58]. Trunk diameters for T1, T2, and T3 are 16.2 cm, 15.8 cm, and 14.4 cm, respectively.

3.4 Spatial distribution of suction around a tree in an urban landscape

3.4.1 Variations in suction at different distances from tree stem

Figure 12a, b shows variations in soil suction (at a minimum depth of 20 cm) at different distances from tree stem

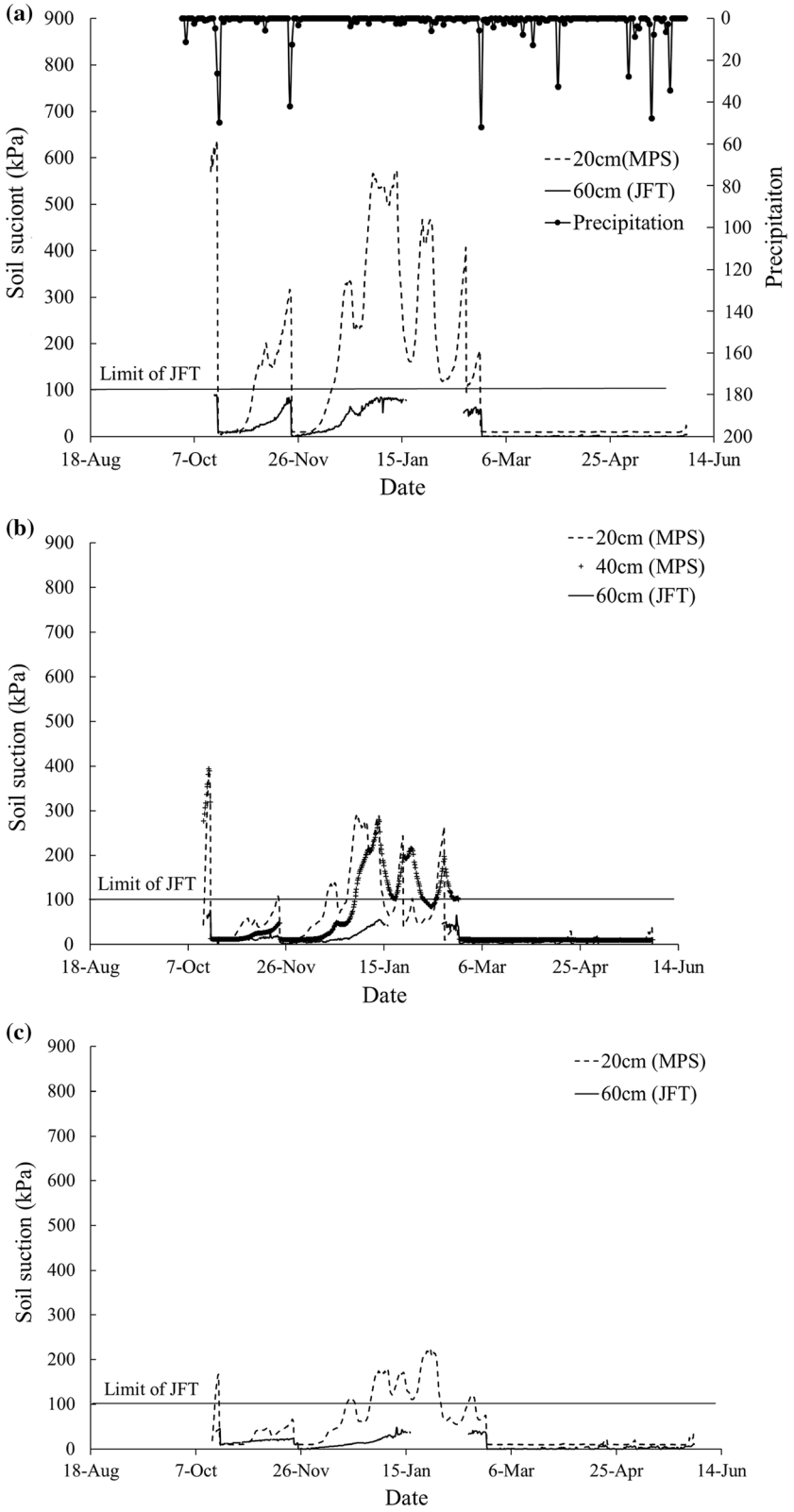

Fig. 13 Variations in soil suction at different depths underground before termite infestation at **a** point A, 0.5 m from tree; **b** point B, 1.5 m from tree; **c** point C, 3 m from tree; and **d** point D, 5.5 m from tree

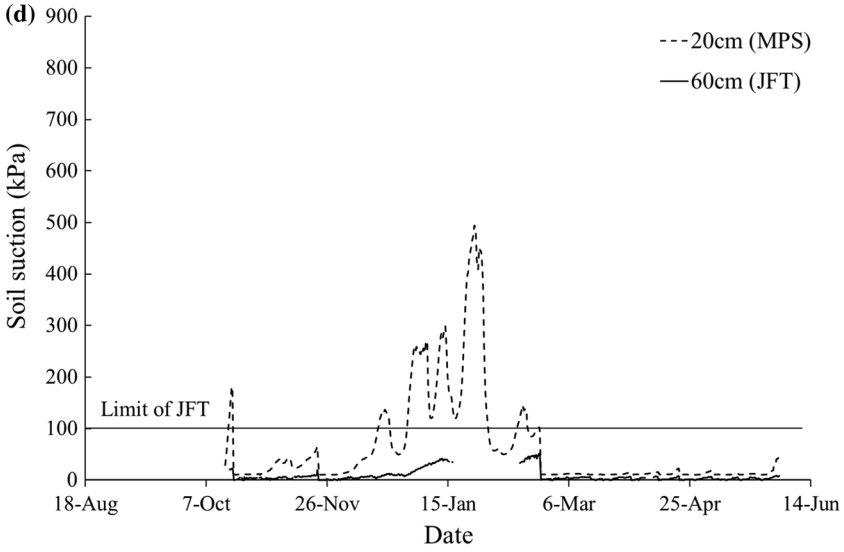

Fig. 13 continued

with time, for stages 1 and 2, respectively. As can be seen, suction magnitude is greatest for the point (A) nearest the tree stem (maximum value of around 629.8 kPa) and lowest for the point (C) farthest from the tree stem. The magnitude of suction at 20 cm depth near the tree stem, however, is lower than that observed for *Schefflera heptaphylla* during summer (at relative humidity of around 70%) when grown on a recompacted slope in a field study under similar climate variations in Hong Kong [19], likely because of the higher relative humidity and lower level of radiant energy observed during the first period of this study: Relative humidity during this period was close to 90% on all but a few days, and air temperature was about 20 °C—much cooler than the average temperature of around 27 °C, with relative humidity of around 70%, observed in the field study conducted by Garg et al. [19]. This is because suction is mainly governed by relative humidity [10]. Beyond March 2017, higher precipitation existed during this field test that reduced suction.

Trends in soil suction over time are not consistent with those for observed radiant energy distribution (refer to Fig. 8; diurnal variation) at different distances from the tree stem, because although radiant energy decreased significantly at night, changes in soil suction were not significant. Because suction is more dependent on relative humidity, brief variations in radiant energy (such as at night) may not be sufficient to cause diurnal variations in suction. Inconsistencies between suction and radiant energy are also observed with respect to distance from the tree stem. Based on observed radiant energy, evapotranspiration rate [as calculated from Penman–Monteith (1986)], and hence induced suction, must have been greater at distances away from tree stem. This contrasting trend is likely related to the dominance of tree root water uptake over evaporation rate. As expected, the dominance is more significant near the tree stem than at farther locations. Moreover, the equation proposed by Penman–Monteith is valid for uniform vegetation cover and ignores any interaction effects from another vegetation species (such as the tree in this study). Although the trend in suction magnitude for points from A to C was also observed in study [12], the comparative is not true, for that study was of a single tree, with no investigation of interaction effects resulting from the presence of other species.

The trend of suction magnitude does not seem to hold for points C and D, with the rate of increase in suction under drying higher at point D than at point C, very likely owing to the dominance of the evaporation effect from the soil surface, itself a result of an increase in radiant energy compared to root water uptake from tree roots. On some occasions, the suction magnitude at point D might be greater than at point A (nearest the tree stem), especially during the rainy season, when the root water uptake effect is minimal. Previous research has shown that the average root system diameter is about 2.9 times the diameter of the canopy [9]. Because points C and D were located at much farther distances (3 m and 5.5 m) from the tree stem, it is highly possible that they fall in either the lowest root density zone or, if possible, none at all, based on the root density distribution profiles of trees [12]. So significant a variation in soil suction in a lateral direction provides crucial information with which to analyze the differential settlement of soil and hence any urban infrastructures around it [34]. It should be also noted that differences in

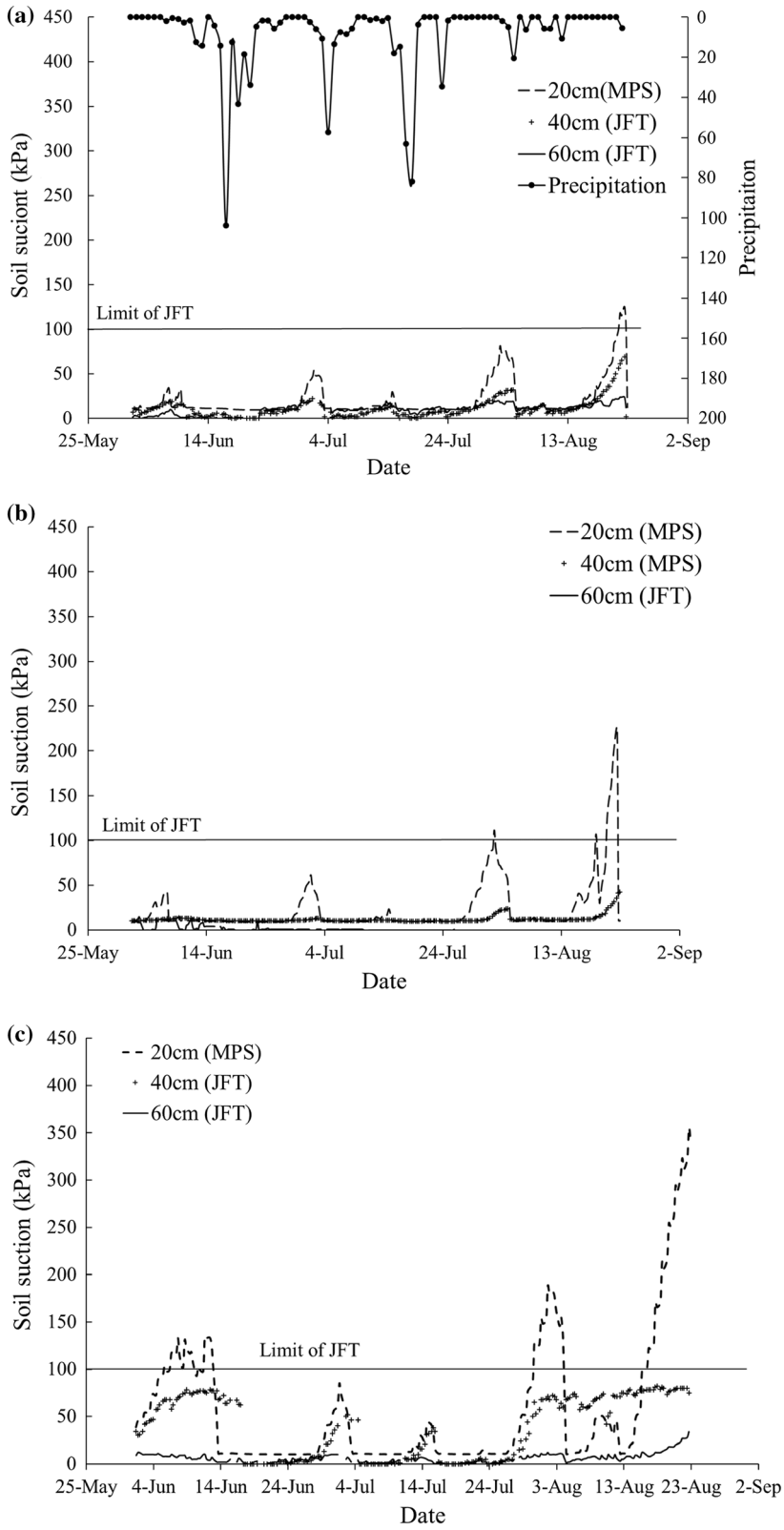

Fig. 14 Variations in soil suction at different distances from tree stem after onset of termite infestation, at **a** point A, 0.5 m from tree; **b** point B, 1.5 m from tree; **c** point C, 3 m from tree; and **d** point D, 5.5 m from tree

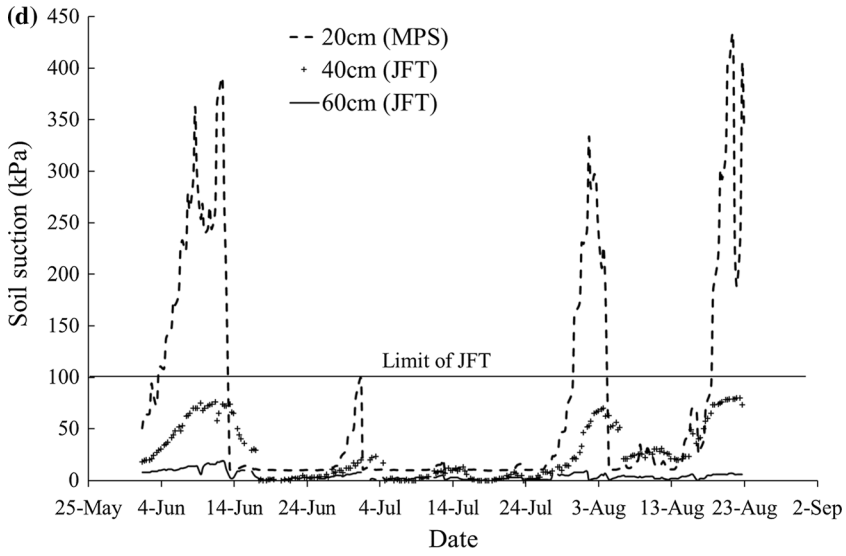

Fig. 14 continued

suction magnitude were negligible during rainy season (beyond March 2017).

By contrast, the second stage of the monitoring period (Fig. 12b) seemed to show a rapid increase in soil suction for point D and even point C compared to the other points. The rise in suction for point C might have resulted from a reduction in canopy interception effects as well as an increase in evaporation effects during summer. This may be because of a combination of several factors, such as increased radiant energy at points C and D (Fig. 9b) and decreased T2 canopy area (Fig. 10; possibly due to termite infestation) as well as stomatal conductance (Fig. 11). The increased radiant energy at points C and D may be because of changes in solar elevation angle (Fig. 8) in the summer, with the sun's radiant energy likely spread over large distances. This indicates that the suction variations in a multiple-tree system in urban areas are highly dependent not only on vegetation canopy growth but also on climate parameters, including solar elevation angle and corresponding radiant energy.

3.4.2 Variations in suction profiles at different depths before termite infestation

To fully understand the spatial distribution of suction in the vicinity of a tree, suction profiles at different depths (i.e., 20 cm, 40 cm, and 60 cm) were plotted for all four points away from the tree stem (Fig. 13a–d). Figure 13 shows variations in suction distribution before the termite infestation, with the magnitude as well as the change in suction (under drying or wetting) much lower at 60 cm deep than at 20 cm. This difference of suction across depths is much larger for the point (A) nearest the tree stem. Although different instrumentation (i.e., jet fill tensiometer) was employed for measuring suction at greater depths, random exchange of instrumentation among different points found trends to be similar. So significant a reduction in suction beyond 20 cm deep seems to suggest very shallow depth, and hence influence zone, of tree roots, perhaps because the trees in question were transplanted to the given site on the University of Macau campus 2 years before the start of monitoring. The root depths during transplantation were around 0.4–0.5 m.

The vertical suction profile is in stark contrast to the observed deeper influence zone of suction by tree root water uptake found in previous field studies [3, 12, 25], likely because in an urban landscape (as in this study), trees are often grown by transplantation on artificially compacted soil; hence root depth is expected to be less during the first few years after transplant. Jim [27] also observed suppression of growth in trees planted along roadsides in Hong Kong, finding that the high shear strength of the soil and the lack of adequate soil depth, water, and nutrient sources were major factors causing reduced tree growth in urban areas. By contrast, soil conditions in forests (including the presence of nutrients) are likely to be more favorable for tree growth.

3.4.3 Variations in suction profiles at different depths after termite infestation

Figure 14 shows variations in vertical suction profiles at different distances from the tree stem (A, B, C, and D) for the monitoring period likely to correspond to the period of

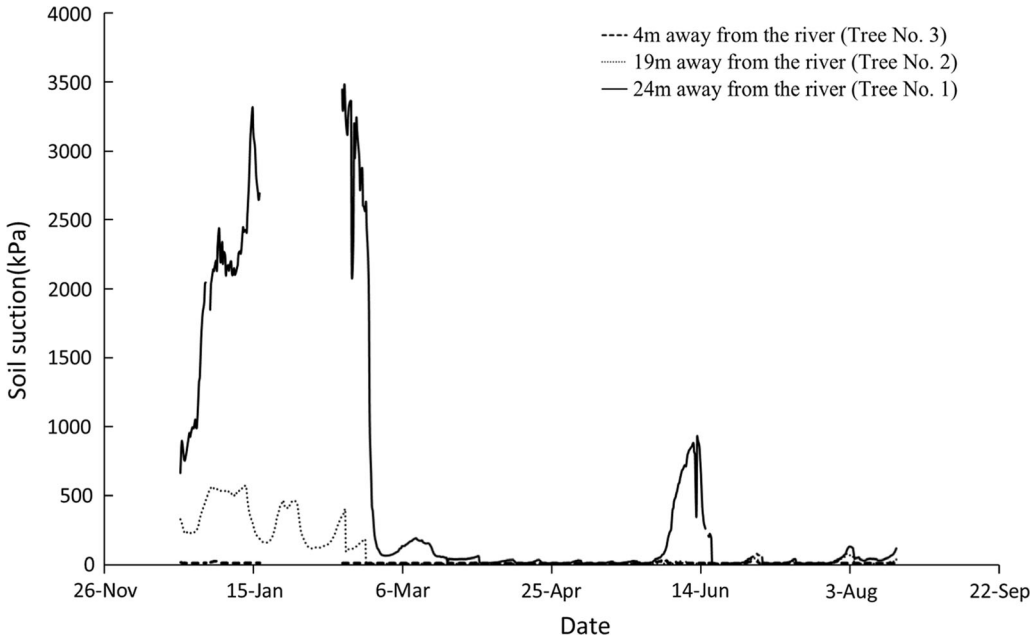

Fig. 15 Variations in soil suction among T1, T2, and T3 at three distances from a river

termite infestation. It can be seen from Fig. 14 that there is significantly reduced soil suction at 20 cm depth during this monitoring period compared to that seen during the earlier monitoring period (Fig. 12). The suction at 20 cm depth near the tree is within 100 kPa (Fig. 14), compared with more than 600 kPa seen during the previous monitoring period (Fig. 13). Interestingly, however, areas distant from the tree (points B, C, and D) were found to have greater suction at 20 cm depth, a trend contrasting with that seen in Fig. 13. It appears from this trend that the effect of root water uptake near the tree was reduced significantly during the second stage of monitoring period. One major factor could be a termite infestation that reduced leaf area (Fig. 10) and stomatal conductance (Fig. 11b). Such a reduction in leaf area would reduce evapotranspiration near the tree stem due to less interception of radiant energy [19] and, hence, induced suction. However, for distances farther from the tree stem, evaporation effects are likely to dominate with further reduction in tree canopy. This is likely to have caused higher induced suctions at 20 cm depths for distances away from tree stem. Increased suction due to a reduction in canopy area has also been observed for species native to Hong Kong [19]. For 40 cm depth, the suction magnitude increased significantly at the distances farthest from the tree stem. Overall, the observed response of suction across different distances from the tree stem indicates that despite climate conditions favorable (in the second stage of the monitoring period) for inducing higher suctions, tree roots were least efficient due to termite infestation. This was also confirmed by the drastic reduction in leaf area (Fig. 10) and stomatal conductance (Fig. 11).

3.4.4 Variations in soil suction induced in trees at different distances from a river

It can be seen from Fig. 15 that soil suction at even 20 cm depth for T3, close to the river, was almost negligible compared to suction induced in T1 and T2, likely because continuous subsurface water flow from the river countered the effect of T3. T1 was observed to induce peak suction almost 7 times that induced by T2, because T1 was farthest from the river and also closer to the building (an impermeable wall), where soil is limited and any competition from other trees for water uptake is negligible. The growth of T1 was expected to exceed that of T2. Also, the trend of induced suction is consistent with average canopy area, which was highest for T1 and lowest for T3. Thus, several factors, including distance from river and canopy area, could influence suction—a possibility needing further investigation. Considering that the main focus of this study is to reveal the effects of termite infestation, future work should study in depth the influence of tree location in the urban landscape on transpiration-induced suction. Also, quantification of termite infestation should be carried out using specially designed techniques [39].

4 Conclusions

In this study, spatial distribution of soil suction was investigated in an urban tree, considering the influences of tree canopy effects and termite infestation. Field monitoring was conducted to monitor suction, climate parameters (radiant energy, relative humidity), and plant parameters, including stomatal conductance and canopy area. A new color analysis technique was developed to estimate canopy area. Spatial variations in suction near the tree were interpreted with respect to measured climate and plant parameters.

It was found that suction (especially at shallow depths) was highest near the tree stem and decreased with distance from the tree stem up to 3 m—an expected result considering the reduction in root density that accompanies distance from tree stem. At this distance, it is also expected that canopy shading effects will be higher, reducing evaporation. However, at 5.5 m (i.e., beyond the canopy), suction at shallow depths again increased, likely because of the dominance of evaporation effects beyond the estimated root spread of around 4.5 m. Interestingly, suction at greater depths (i.e., 0.6 m) did not vary significantly with distance from tree stem, implying that tree canopy shading effects are effective only within the root zone (i.e., 0.4–0.5 m).

However, termite infestation seems to have significantly influenced suction. Suction at shallow depths was found to reduce significantly due to decreased canopy area and stomatal conductance induced by infestation of a tree. The relation of suction to distance from tree stem also changed after termite infestation, with evaporation effects becoming dominant due to reductions in canopy area. Accordingly, suction at shallow depths was found to increase with distance from the tree stem, in contrast to the effect observed during the initial monitoring period. In summary, this study revealed the effects of termite infestation on tree growth and soil suction—and because these effects are significant, this phenomenon should be considered when adopting a policy for maintaining green infrastructure (slopes, urban landscape, landfill covers, etc.). Considering that the main focus of this study was the analysis of soil suction near urban trees, further comprehensive studies are required (in both controlled and uncontrolled environments) to quantify the effects of termite infestation on soil suction and performance of green infrastructure. Further systematic studies are required to utilize techniques of machine learning and probabilistic analysis [22, 23].

Acknowledgements The authors gratefully acknowledge financial support from the University of Macau Research Fund (MYRG2018-00173-FST; MYRG2015-00112-FST) and the Macau Science and Technology Development Fund (FDCT) (Code: 193/2017/A3). The authors would also like to thank Shantou University Scientific Research Fund (NTF17007) for support.

References

1. Allen RG, Pereira LS, Raes D, Smith M (1998) Crop Evapotranspiration guidelines for computing Crop Water Requirements. FAO Irrigation and Drainage Paper 56. FAO, Rome
2. Aasamaa K, Sõber A (2011) Responses of stomatal conductance to simultaneous changes in two environmental factors. Tree Physiol 31(8):855–864
3. Biddle PG (1983) Patterns of soil drying and moisture deficit in the vicinity of trees on clay soils. Geotechnique 33(2):107–126
4. Bush SE, Pataki DE, Hultine KR, West AG, Sperry JS, Ehleringer JR (2008) Wood anatomy constrains stomatal responses to atmospheric vapor pressure deficit in irrigated, urban trees. Oecologia 156(1):13–20
5. Bhatt R, Arora S, Chew CC (2016) Improving irrigation water productivity using Tensiometers. J Soil Water Conserv 15(2):120–124
6. Briggs K, Smethurst JA, Powrie W, O'Brien AS (2016) The influence of tree root water uptake on the long term hydrology of a clay fill railway embankment. Transp Geotech 9:31–48
7. Bordoloi S, Hussain R, Gadi VK, Bora H, Sahoo L, Karangat R, Garg A, Sreedeep S (2018) Monitoring soil cracking and plant parameters for a mixed grass species. Géotechn Lett 8(1):49–55
8. Decagon Devices (2014) Commercial publications, operator's manual for MPS-2 & MPS-6 dielectric water potential sensors. Decagon Devices, Inc., Pullman www.decagon.com. Accessed 18 Dec 2015
9. Elkins NZ, Sabol GV, Ward TJ, Whitford WG (1986) The influence of subterranean termites on the hydrological characteristics of a Chihuahuan desert ecosystem. Oecologia 68:521–528
10. Edlefsen N, Anderson A (1943) Thermodynamics of soil moisture. Calif Agric 15(2):31–298
11. Fanshawe DB (1968) The vegetation of Zambian termitaria. Kirkia 6(2):169–179
12. Fatahi B, Khabbaz H, Indraratna B (2010) Bioengineering ground improvement considering root water uptake model. Ecol Eng 36(2):222–229
13. Garnier-Sillam E, Harry M (1995) Distribution of humic compounds in mounds of some soil-feeding termite species of tropical rainforests: its influence on soil structure stability. Insectes Soc 42:167–185
14. Gomes MDMDA, Lagôa AMMA, Medina CL, Machado EC, Machado MA (2004) Interactions between leaf water potential, stomatal conductance and abscisic acid content of orange trees submitted to drought stress. Braz J Plant Physiol 16(3):155–161
15. Gadi VK, Bordoloi S, Garg A, Kobayashi Y, Sahoo L (2016) Improving and correcting unsaturated soil hydraulic properties with plant parameters for agriculture and bioengineered slopes. Rhizosphere 1:58–78
16. Gadi VK, Bordoloi S, Garg A, Sahoo L, Berretta C, Sekharan S (2017) Effect of shoot parameters on cracking in vegetated soil. Environ Geotech 5(2):1–31
17. Gadi VK, Tang YR, Das A, Monga C, Garg A, Berretta C, Sahoo L (2017) Spatial and temporal variation of hydraulic conductivity and vegetation growth in green infrastructures using infiltrometer and visual technique. CATENA 155:20–29
18. Gadi VK, Bordoloi S, Garg A, Sahoo L, Berretta C, Sekharan S (2018) Effect of shoot parameters on cracking in vegetated soil. Environ Geotech 5(2):1–31

19. Garg A, Leung AK, Ng CWW (2015) Comparisons of soil suction induced by evapotranspiration and transpiration of *S. heptaphylla*. Can Geotech J 52(12):2149–2155
20. Garg A, Coo JL, Ng CWW (2015) Field study on influence of root characteristics on soil suction distribution in slopes vegetated with *Cynodon dactylon* and *Schefflera heptaphylla*. Earth Surf Proc Land 40(12):1631–1643
21. Garg A, Leung AK, Ng CWW (2015) Transpiration reduction and root distribution functions for a non-crop species *Schefflera heptaphylla*. CATENA 135:78–82
22. Garg A, Hazra B, Zhu H, Wen Y (2019) A simplified probabilistic analysis of water content and wilting in soil vegetated with non-crop species. Catena 175:123–131
23. Gopal P, Bordoloi S, Ratnam R et al. (2019) Investigation of infiltration rate for soil-biochar composites of water hyacinth. Acta Geophys 67:231
24. Hazra B, Gadi V, Garg A, Ng CWW, Das GK (2017) Probabilistic analysis of suction in homogeneously vegetated soils. CATENA 149:394–401
25. Hemmati S, Gatmiri B, Cui YJ, Vincent M (2012) Thermo-hydro-mechanical modelling of soil settlements induced by soil-vegetation-atmosphere interactions. Eng Geol 139:1–16
26. Iwasaki H (2006) Impact of interannual variability of meteorological parameters on vegetation activity over mongolia. J Meteorol Soc Jpn 84:745–762
27. Jim CY (1997) Roadside trees in urban Hong Kong: part IV tree growth and environmental condition. Arboric J 21(2):89–106
28. Jouquet P, Ngo Thi P, Nguyen H, Henry-des-Tureaux T, Chevallier T, Tran Duc T (2011) Laboratory investigation of organic matter mineralization and nutrient leaching from earthworm casts produced by *Amynthas khami*. Appl Soil Ecol 47:24–30
29. Kaye JP, McCulley RL, Burke IC (2005) Carbon fluxes, nitrogen cycling, and soil microbial communities in adjacent urban, native and agricultural ecosystems. Glob Change Biol 11(4):575–587
30. Kuuluvainen T, Pukkala T (1989) Simulation of within-tree and between-tree shading of direct radiation in a forest canopy: effect of crown shape and sun elevation. Ecol Model 49(1–2):89–100
31. Kho MR (2000) A general tree-environment-crop interaction equation for predictive understanding of agroforestry systems. Agric Eco-syst Environ 80(1–2):87–100
32. Lamoureux S, O'Kane MA (2012) Effects of termites on soil cover system performance. Mine closure. Australian Centre for Geotechnics, pp 433–446
33. Leuzinger S, Vogt R, Körner C (2010) Tree surface temperature in an urban environment. Agric For Meteorol 150(1):56–62
34. Li J, Guo L (2017) Field investigation and numerical analysis of residential building damaged by expansive soil movement caused by tree root drying. J Perform Constr Facil 31(1):D4016003
35. Lindberg F, Grimmond CSB (2011) The influence of vegetation and building morphology on shadow patterns and mean radiant temperatures in urban areas: model development and evaluation. Theor Appl Climatol 105(3–4):311–323
36. Malaisse F, Anastassiou-Socquet F (1977) Contribution à l'étude de l'écosystème forêt claire (miombo): Note 24: Phytogéographie des hautes termitières du shaba méridional (zaïre). Bulletin de la Société Royale de Botanique de Belgique/Bulletin van de Koninklijke Belgische Botanische Vereniging, pp 85–95
37. Mitchell JD (2002) Termites as pests of crops, forestry, rangeland and structures in Southern Africa and their control. Sociobiology 40(1):47–69
38. McDonnell MJ, Pickett ST, Groffman P, Bohlen P, Pouyat RV, Zipperer WC, Medley K (1997) Ecosystem processes along an urban-to-rural gradient. Urban Ecosyst 1(1):21–36
39. Monteith JL (1981) Evaporation and surface temperature. Q J R Meteorol Soc 107(451):1–27
40. Möller M, Assouline S (2007) Effects of a shading screen on microclimate and crop water requirements. Irrig Sci 25(2):171–181
41. Moreno F, Cayuela JA, Fernández JE, Fernández-Boy E, Murillo JM, Cabrera F (1996) Water balance and nitrate leaching in an irrigated maize crop in SW Spain. Agric Water Manag 32(1):71–83
42. Ng CWW, Garg A, Leung AK, Hau BCH (2016) Relationships between leaf and root area indices and soil suction induced during drying–wetting cycles. Ecol Eng 91:113–118
43. Ng CWW, Ni JJ, Leung AK, Zhou C, Wang ZJ (2016) Effects of planting density on tree growth and induced soil suction. Géotechnique 66(9):711–724
44. Ni JJ, Cheng YF, Bordoloi S, Bora H, Wang QH, Ng CWW, Garg A (2018) Investigating plant root effects on soil electrical conductivity: An integrated field monitoring and statistical modelling approach. Earth Surf Process Landforms. https://doi.org/10.1002/esp.4533
45. Rogers LKR, French JRJ, Elgar MA (1999) Suppression of plant growth on the mounds of the termie *Coptotermes lacteus* Froggatt (Isopetra, Rhinotermitidae). Insectes Soc 46:366–371
46. Rahardjo H, Satyanaga A, Leong EC, Santoso VA, Ng YS (2014) Performance of an instrumented slope covered with shrubs and deep-rooted grass. Soils Found 54(3):417–425
47. Sellers PJ (1985) Canopy reflectance, photosynthesis and transpiration. Int J Remote Sens 6(8):1335–1372
48. Smethurst JA, Clarke D, Powrie W (2012) Factors controlling the seasonal variation in soil water content and pore water pressures within a lightly vegetated clay slope. Géotechnique 62(5):429–446
49. Smethurst JA, Clarke D, Powrie W (2006) Seasonal changes in pore water pressure in a grass covered cut slope in London clay. Géotechnique 56(8):523–537
50. Switala BM, Wu W (2015) Numerical simulations of the mechanical contribution of the plant roots to slope stability. In: Wu W (ed) Recent advances in modeling landslides and debris flows. Springer International Publishing, Cham, pp 265–274. ISBN 978-3-319-11052-3
51. Switala BM, Askarinejad A, Wu W, Springman SM (2018) Experimental validation of a coupled hydro-mechanical model for vegetated soil. Géotechnique 68(5):375–385
52. Tripathy S, Al-Khyat S, Cleall PJ, Baille W, Schanz T (2016) Soil suction measurement of unsaturated soils with a sensor using fixed-matrix porous ceramic discs. Indian Geotech J 46(3):252–260
53. Tardieu F, Katerji N, Bethenod O, Zhang J, Davies WJ (1991) Maize stomatal conductance in the field: its relationship with soil and plant water potentials, mechanical constraints and ABA concentration in the xylem sap. Plant Cell Environ 14(1):121–126
54. Temps RC, Coulson KL (1977) Solar radiation incident upon slopes of different orientations. Sol Energy 19(2):179–184
55. Wang FX, Kang Y, Liu SP, Hou XY (2007) Effects of soil matric potential on potato growth under drip irrigation in the North China Plain. Agric Water Manag 88(1):34–42
56. Wu W, Switala BM, Acharya MS, Tamagnini R, Auer M, Graf F, Kamp LT, Xiang W (2015) Effect of vegetation on stability of soil slopes: numerical aspect. In: Wu W (ed) Recent advances in modeling landslides and debris flows. Springer International Publishing, Cham, pp 163–177. ISBN 978-3-319-11052-3
57. Xu XQ, Su LJ, Zhang GD, Zhu HH (2017) Analysis on shear wave velocity structure of a gravel landslide based on dual-source surface wave method. Landslides 14:1127–1137
58. Zhang QH, Byers JA, Zhang XD (1993) Influence of bark thickness, trunk diameter and height on reproduction of the longhorned beetle, *Monochamus sutor* (Col., Cerambycidae) in burned larch and pine. J Appl Entomol 115(1–5):145–154

59. Zhou WH, Yuen KV, Tan F (2014) Estimation of soil-water characteristic curve and relative permeability for granular soils with different initial dry densities. Eng Geol 179:1–9
60. Zhou WH, Garg A, Garg A (2016) Study of the volumetric water content based on density, suction and initial water content. Measurement 94:531–537
61. Zhan TLT, Chen R, Ng CW (2014) Wetting-induced softening behavior of an unsaturated expansive clay. Landslides 11(6):1051–1061